Effect of Cracks on the Dielectric Breakdown of Polymers and Ceramics

Raúl Pech-Pisté, Francis Avilés, Zarel Valdez-Nava, David Malec

Effect of cracks on the dielectric breakdown of polymers and ceramics

Raúl Pech Pisté[1,2], Francis Avilés[1,2*], Zarel Valdez-Nava[2], David Malec[2]

[1]*Materials Department, Centro de Investigación Científica de Yucatán A.C.,* Mérida, Mexico
[2]*LAPLACE, Université de Toulouse, CNRSm INTP, UPS,* Toulouse, France

*faviles@cicy.mx

***Abstract*—The influence of an insulating crack on the dielectric breakdown of polymers and ceramics is evaluated by finite element modeling. Measured dielectric breakdown and relative permittivity for epoxy resin and alumina specimens were used as inputs for the numerical model. An insulating crack was modelled in the center of the material, with its longitudinal direction aligned parallel and perpendicular to the electric field direction. The intensity of the electric field increases up to 17 times, confined within the crack when the crack was perpendicular to the field. The presence of a crack parallel to the field does not cause large disturbances on the electrical field distribution. The measured dielectric breakdown for both materials were similar to those obtained by the model with the crack in perpendicular direction.**

Keywords—dielectric breakdown, alumina, epoxy resin, finite element modelling

I. Introduction

Polymers and ceramics are widely used as packaging materials for electronic devices, ranging from low to high voltage applications. However, these insulating materials are susceptible to electrical breakdown, which is a critical parameter affecting the reliability and lifespan of such devices. The breakdown process is complex and not fully understood, as it may involve multiple coupled effects such as thermal, mechanical, and electrical phenomena. Various mechanisms have been proposed to describe the breakdown process of solid dielectrics, with the most studied models being electrical, thermal, and electromechanical ones [1].

By definition, electromechanical breakdown occurs when the electrostatic attraction between charged particles exceeds the elasticity of the dielectric material. The high electric fields can induce microscopic damage, leading to mechanical failure due to electrical and mechanical interactions. Several analyses have suggested that the presence of pre-existing cracks within the material plays a significant role. Principles of fracture mechanics and analogies to it have demonstrated a relationship between dielectric strength, and the defects within the material [2-6]. Therefore, understanding the role of pre-existing cracks on the dielectric breakdown of solid dielectrics is crucial for designing reliable insulating systems [2].

This study aims to investigate, both theoretically and experimentally, the influence of initial cracks on the dielectric breakdown of polymers and ceramics subjected to high voltages. The finite element model (FEM) is a progressive electrostatic model in which the material (dielectric) properties corresponding to each voltage are sequentially considered for the next incremental voltage step. Even when this simplified model does not account for mass transport or dynamic effects, it is shown here that it is able to capture the fundamental governing physics of dielectric cracks and explain the experimental results.

II. Methods

A. Experimental characterization of dielectric properties

The input values for the FEM were obtained from the dielectric characterization of a commercial alumina and a home-synthesized epoxy polymer. The epoxy polymer RE 7000-1 (bisphenol-A and epichlorohydrin), along with its crosslinking agent HD 307 (alkylated phenols and polyoxypropylenediamine) were acquired from Poliformas Plásticas (Mérida, Mexico). α-Al_2O_3 plates with thickness of 1 mm were sourced from CeramTec (Plochigen, Germany).

Dielectric breakdown tests were conducted in a DPA 75C oil breakdown voltage tester (BAUR, Austria) equipped with spherical electrodes of 12.7 mm in diameter. Square specimens with in-plane dimensions of 25 mm x 25 mm, and 1 mm thickness were subjected to a sinusoidal 50 Hz alternating current signal with a voltage ramp of 1.5 kV/s for Al_2O_3 and 3.0 kV/s for epoxy polymer. Specimens were immersed in a dielectric fluid (Galden HT55) to avoid surface flashover. Dielectric properties of both materials were obtained by analyzing the phase shift of the voltage and current signals in a frequency (f) range of 10^{-2} to 10^{6} Hz at an applied voltage of 1 V. For this purpose, an Alpha-A broadband dielectric spectrometer (Novocontrol Technologies, Montabaur, Germany) was used. Both materials were cut in squared shapes with dimensions of 25 mm x 25 mm. Then, a ~50 nm-thickness gold electrode was defined in both surfaces of each sample. Tests were performed at room temperature (~25 °C) and three replicates of each material were tested.

B. Finite element modelling

A progressive FEM was developed to analyze the effect of a crack on the electric field distribution in epoxy and alumina specimens. This electrostatic model was simulated by solving the Poisson's equation using the software ANSYS®. Although the analysis of this problem in a three-dimensional scenario should be more realistic, a two-dimensional domain was selected for improve the efficiency of calculations. The two-dimensional simplification might not yield the same electric field intensity, but the same electric field distribution [7]. Therefore, the geometry of the model simulates a slice of the through-thickness direction (xz plane) of specimens used in dielectric breakdown tests. The model is two-dimensional, and the geometry consists of a rectangular cross-sectional area with dimensions of 25 mm x 1 mm, composed of 24 areas, and 63,240 quadratic elements (PLANE230). An initial crack with dimensions of a = 500 μm and b = 10 μm and specific material properties (see Table I) was placed at the center of the plate specimen, as shown in the inset in Figure 1.

The mesh of the model was graded (refined) according to the proximity to the crack tip. A refined mesh zone (RMZ) of 1500 μm was defined after a dedicated analysis. This zone

contained the smallest elements (SE), 10 µm x 10 µm, and covers the distance of the crack length plus a distance where the parameters of interest are not expected to change. Outside this zone, the specimen was meshed with larger elements (LE) of 50 µm x 10 µm to simulate the far-field zone. A convergence analysis was conducted to determine the independence of the results with the number of elements.

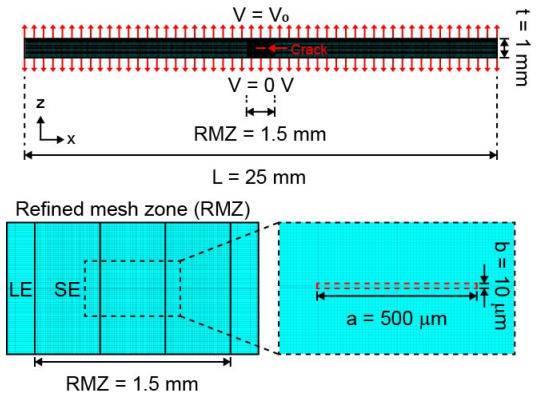

Fig. 1 Electrical FEM of dielectric breakdown of a plate specimen containing a crack.

The electrical field was applied along the through-thickness (*z*-direction) by fixing a potential difference between the two longitudinal edges of the modeled specimens, with $V = 0$ V at the bottom edge, and $V = V_0$ at the top edge. The model was evaluated under DC voltages, and dynamic effects were not included. In each step, the voltage was increased according to the voltage ramp used in the experimental part. After each voltage step, the electrical field and current density were extracted, focusing on their local gradients around the crack.

Dielectric breakdown can be treated as a local change of conductivity when a voltage applied through an insulator exceeds a threshold [8,9]. Thus, the dielectric breakdown was modeled by changing the local material properties (electrical conductivity and relative permittivity) of elements that exhibit electrical field gradients higher than the dielectric breakdown value obtained experimentally, as described in Figure 2.

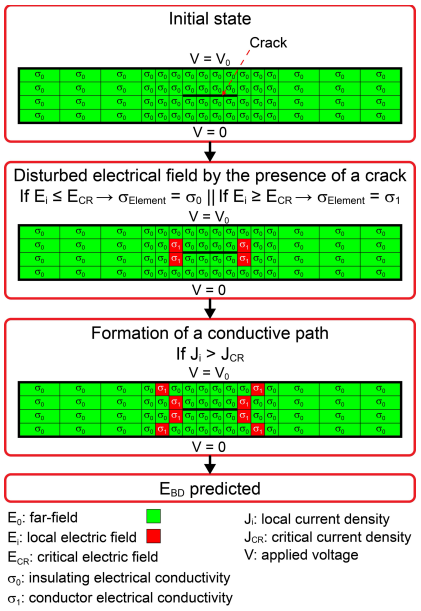

Fig. 2 Flowchart of the progressive electrical FEM.

At the initial state, the model possesses elements with only two different material properties, i. e., the electrical conductivity and relative permittivity of the material (epoxy resin or Al_2O_3), and those of the insulating crack. After the application of V_0, the local electric field value in each element (E_i) was compared with a critical electric field value (E_{CR}), which herein corresponds to the measured dielectric breakdown field. This is set to 42.6 x10^6 V/m for the epoxy resin, and 23.6 x10^6 V/m for Al_2O_3. If $E_i < E_{CR}$, the electrical properties of the elements maintain its original value. If $E_i \geq E_{CR}$, the electrical properties of the material change to a third value corresponding to a conductive material, yielding an element with a non-negligible local current density. The model iterates by increasing the voltage until V_0 reaches E_{CR}, i.e., the measured breakdown voltage value. At this point, the effect of the crack in the electric field and current density distribution is observed. Table 1 summarizes the electrical properties of the epoxy and Al_2O_3, obtained from the experimental part of this work. The crack was simulated as an insulating material with the electrical properties of air [10].

TABLE I. MATERIALS PROPERTIES USED IN THE FEM MODEL

Material	Property	
	Electrical resistivity (Ω·m)	*Relative permittivity*
Epoxy resin	1 x10^{12}	5.5
Al_2O_3	1 x10^{13}	12
Crack (air)	1 x 10^{14}	1
Conductive material	1 x10^{-1}	10

Finally, the effect of the orientation of the crack was evaluated by simulating a crack of the same length but oriented at 0° (parallel) with respect to the applied electric field.

III. Results and Discussion

A. *Dielectric properties of epoxy and Al_2O_3 specimens*

The epoxy specimens (E_{BD} = 42.6 kV/mm) present a higher dielectric breakdown mean value than the Al_2O_3 specimens (E_{BD} = 23.6 kV/mm). This difference can be attributed to the molecular structure of the materials [11]. Thermosetting polymers have a structure composed of cross-linked networks of long molecular chains with atoms covalently bonded. As a consequence, polymers lack free mobile charges, making more difficult the conduction of electrons. Although the alumina structure also lacks free mobile charges, ionic structure makes it fragile and more prone to dielectric breakdown. Values of dielectric breakdown of both materials are similar to those reported in literature, viz. 25-45 kV/mm for epoxy [12] and 26 kV/mm for Al_2O_3 [13].

Regarding the broadband dielectric spectroscopy, for $f < 10^2$ Hz, the real part of the complex electrical conductivity (σ_e') exhibited a linearly increasing response varying from ~10^{-13} S/m at 10^{-2} Hz to ~10^{-9} S/m at 10^2 Hz for both materials. For $f > 10^2$ Hz, a non-linear behavior of σ_e' is observed for both epoxy and Al_2O_3, with a more remarkably change of slope for the later one. This characteristic is an indicative of a capacitive contribution and depends on the frequency range.

The real part of the relative permittivity slightly decreased as a function of frequency. The input values for the electrical conductivity and relative permittivity used in the FEM (Table I) corresponded to those measured at $f = 10^{-2}$ Hz.

B. *Electrical finite element model of a crack perpendicular to the electric field*

Figure 3 displays the results of the electrical FEM of an epoxy specimen with a crack perpendicular to the direction of the electric field at two voltage steps. The figure depicts an overall view of the complete specimen with close ups at the crack region. These close ups correspond to the complete thickness and 0.06 of the specimen length. The left close ups correspond to the isocontour maps of electric field (E), normalized with respect to the electric field in the far-field, i.e., the electric field in the absence of the crack (E_0). The right close ups correspond to the distribution of the total current density (J) normalized with respect to a critical current density (J_{CR}). J_{CR} was chosen as 10 % of the current density of the conductive material listed in Table I.

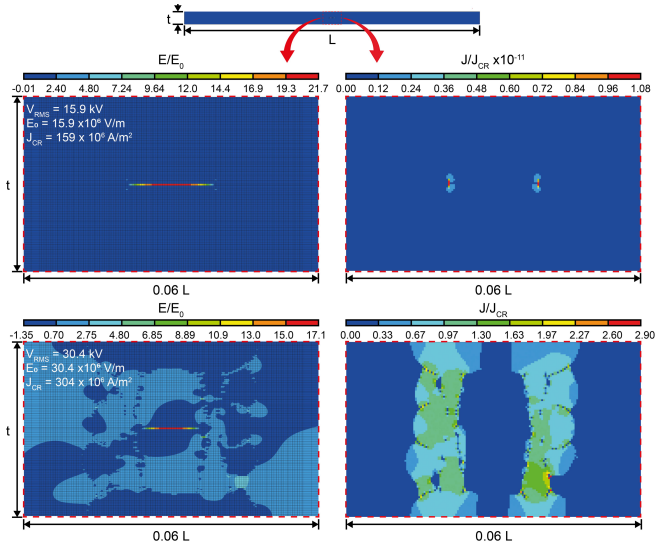

Fig. 3 Normalized electric field and current density distributions of an epoxy specimen with a crack perpendicular to the applied electric field at two voltage steps.

For V_0 from 0 V to 14.8 kV, the electric field present maximum values confined inside the crack. This is consistent with previous observations for an insulating crack [10]. Some small gradients of electric field appeared near the crack tip and increased in magnitude after each step of voltage. For V_0 = 14.8 kV, some elements around the crack tips reached values that overcome E_{CR} (42.7 kV/mm), and thus, changed its electrical properties (electrical resistivity and relative permittivity) to those of a conductive material (see Table I) for the next iteration. For V_0 = 15.9 kV, the electric field at the crack tips was 2.40 to 4.80 times the value of the electric field of the far-field. J/J_{CR} also greatly increased on those elements that became more conductive, forming a small path outside of the crack with values between 0.12 x10^{-12} and 1.08 x10^{-12}. After each step, more elements in the model locally surpassed E_{CR} and changed its properties to conductive ones, and the electric field intensity gradients occupied a larger region of the thickness of the specimen. In certain instances, a few elements near one of the crack tips exhibited electric field values that nearly reach the threshold, while in the other tip, the elements slightly surpass this value. This initiates the growth of an asymmetric pattern along the conductive channel, becoming more pronounced after each voltage step.

For V_0 = 30.4 kV, J/J_{CR} increases up to 11 orders of magnitude higher than those found at V_0 = 15.9 kV (10^{-12}), and the elements formed a sequential conductive path through the whole thickness of the specimen. The formation of the conductive path at this voltage step, corresponding to a peak value of 42.5 kV/mm, is in reasonable agreement with the measured breakdown voltage, 42.7 kV/mm. This indicates that a perpendicular crack causes enough perturbations to the electric field and eventually yields dielectric breakdown.

Figure 4 presents the normalized electrical field distribution and current density distributions of the Al_2O_3 model with a crack perpendicular to the applied electric field at two voltage steps.

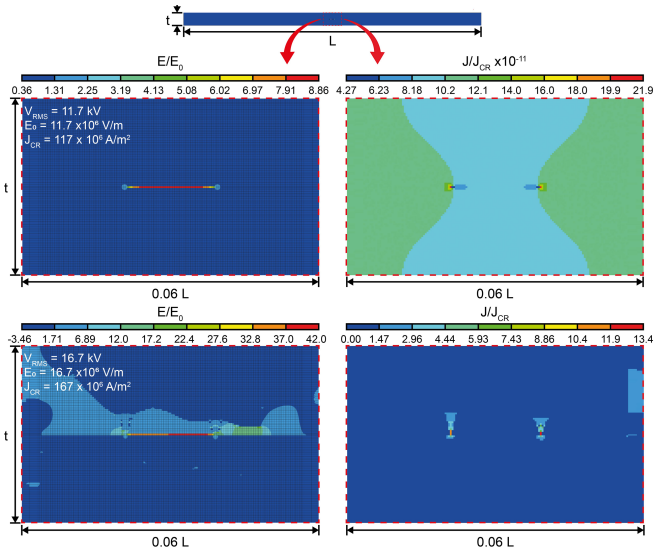

Fig. 4 Normalized electric field and current density distributions of an Al_2O_3 specimen with a crack perpendicular to the applied electric field at two voltage steps.

The electric field also presented the highest values confined within the insulating crack, which extends to the crack tips. After V_0 = 11.7 kV, a few elements reached field values higher than E_{CR} and its conductivity/relative permittivity was changed. For V_0 = 16.7 kV (nearest to the experimental value of dielectric breakdown), E/E_0 was up to 12 times higher than the far-field in some regions outside the crack. J/J_{CR} exhibited the highest values at the crack tips (13.4) and some highly conductive pathways are formed. However, the crack does not cause enough perturbations in the electric field since the branches in J/J_{CR} does not cross the whole thickness of the specimen. Further efforts will be conducted to adjust the dielectric breakdown criteria to better reproduce the obtained experimental data.

C. *Electrical finite element model of a crack parallel to the electric field*

Figure 5 presents the results of the FEM of an epoxy specimen with a crack parallel to the electric field direction at two voltage steps. For V_0 from 1.06 to 29.3 kV, the electric field distribution was not greatly disturbed by the presence of the crack. After V_0 = 29.3 kV, a few elements overcome E_{CR} and thus at that point their material properties were changed to that of the conductive material. At this V_0 value, some small perturbations of the electric field were observed, as well as an increase in the current density at the crack tips. For V_0 = 37.5 kV, the conductive elements crossed the thickness of the specimen and J/J_{CR} increased abruptly to values between 0.05 and 0.43, indicating that J values are in the same order of J_{CR}. This value of E, however, is much higher than the breakdown field measured in the experiments, 42.7

kV/mm. This means that such modeling scenarios are not likely be seen in practice, and the presence of cracks parallel to the electric field are not a paramount factor on the dielectric strength of solid dielectrics. This finding has been qualitatively suggested by Zuo [14].

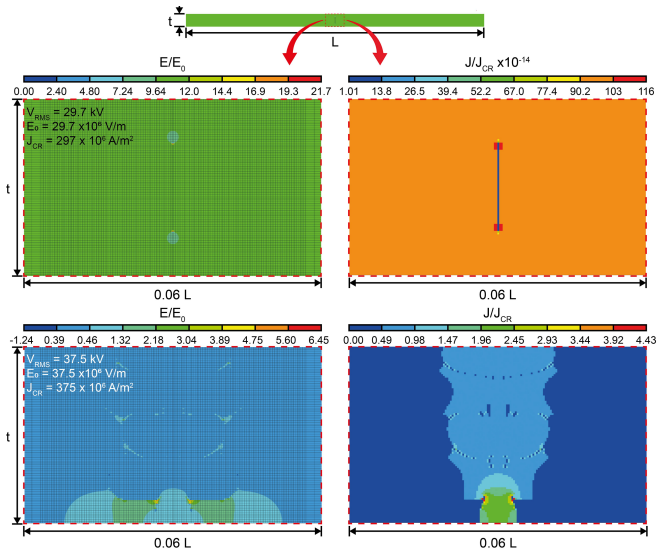

Fig. 5 Normalized electric field and current density distributions of an epoxy specimen with a crack parallel to the applied electric field at two voltage steps.

IV. Conclusions and Perspectives

The influence of cracks on the dielectric breakdown of dielectric materials was evaluated by finite element modeling and experiments. The simulations indicate that the presence of insulating cracks perpendicular to the direction of the applied electrical field yields high local field gradients near the crack tip. At or near the dielectric breakdown, the electric field is magnified up to 17 times for an epoxy specimen and around 12 times for the Al_2O_3 specimen. Assuming that local material around the crack becomes electroconductive when such magnified electric field is locally higher than a critical electric field, conductive paths were found at a voltage that correlates well with the measured voltage breakdown for the epoxy. For Al_2O_3, incipient conductive pathways were formed emanating from the crack tips at electric fields close to the one corresponding to the measured electrical breakdown, but these paths did not cross the full thickness of the specimen. Further modeling considerations are needed to accurately predict the dielectric breakdown of ceramics. This could be using a criterion of critical local dielectric breakdown field arising from analytical models that included cracks, rather than from experimental values. The unavoidable presence of small flaws and/or defects could affect the material's capability to withstand the electrical field. In this sense, the development of an electromechanical model that simulates the interaction of the electric field with cracks and stress concentrations should be considered as alternative modeling strategies.

On the other hand, if the crack is parallel to the electric field direction, the interaction with the applied electric field is small, suggesting that insulating parallel cracks do not present a limiting factor for the design against dielectric breakdown.

The analysis of different parameters of the crack will be of great importance to evaluate its influence on the dielectric strength of materials. Conductive cracks created by the presence of moisture, effects of directionality, size, and shape of the cracks, as well as the interaction of several cracks are parameters that should be investigated.

For alumina, the effect of grain size and grain distribution may be an important contributing factor. Further experiments and simulations will be conducted to evaluate the influence of pre-existing cracks on the dielectric breakdown of solid dielectrics.

Acknowledgment

The authors thank Miguel Rivero for help with specimen preparation.

References

[1] M. X. Zhu, H. G. Song, J. C. Li, et al. "Phase-field modeling of electric-thermal breakdown in polymers under alternating voltage" Transactions on Dielectrics and Electrical Insulation, vol. 27, pp. 1128-1135, 2020.

[2] R. M. McMeeking. "On mechanical stresses at cracks in dielectrics with application to dielectric breakdown" Journal of Applied Physics, vol. 62, pp. 3116-3122, 1987.

[3] E. J. Garboczi. "Linear dielectric-breakdown electrostatics" Physical Review B, vol. 38, pp. 9005-9010, 1988.

[4] J. C. Fothergill. "Filamentary electromechanical breakdown" Transactions on Dielectrics and Electric Insulation, vol. 26, pp. 1124-1129, 1991.

[5] H. G. Beom and Y. H. Kim. "Application of J integral to breakdown analysis of a dielectric material" International Journal of Solids and Structures, vol. 45, pp. 6045-6055, 2008.

[6] G. A. Schneider. "A Griffith type energy release rate model for dielectric breakdown under space charge limited conductivity" Journal of the Mechanics and Physics of Solids", vol. 61, pp. 78-90, 2013.

[7] Y. Sun, L. Yang, G. Shang, Z. Kuang, Y. Liao, Y. Hao, L. Li. "Effects of dynamic deformation of pendant water drops on the electric field between hollow porcelain insulator shed under extreme rainfall" High Voltage, vol. 7, pp. 86-97, 2021.

[8] H. J. Wiesmann and H. R. Zeller. "A fractal model of dielectric breakdown and prebreakdown in solid dielectrics" Journal of Applied Physics, vol. 60, pp. 1770-1773, 1986.

[9] S. Noguchi, M. Nakamichi and K. Oguni. "Proposal of finite element analysis method for dielectric breakdown based on Maxwell's equations" Computational Methods in Applied Mechanical Engineering, vol. 371, pp. 2-14, 2020.

[10] S. Naderi, J. P. Heath and J. S. Dean. "Morphology characterisation of inclusions to predict the breakdown strength in electro-ceramic materials: Microstructre modelling" Ceramics International, vol. 45, pp. 361-368, 2019.

[11] M. Ieda. "Dielectric breakdown process of polymers" Transactions on Dielectrics and Electrical Insulation, vol. 15, pp. 206-224, 1980.

[12] K. Yang, W. Chen, Y. Zhao, et al. "Enhancing dielectric strength of thermally conductive epoxy composites by preventing interfacial charge accumulation using micron-sized diamond" Composites Science and Technology, vol. 221, pp. 109178, 2022.

[13] D. Malec, V. Bley, F. Talbi, F. Lalam. "Contribution to the undestanding of the relationship between mechanical and dielectric strengths of alumina" Journal European of Ceramic Society, vol. 30, pp. 3117-3123, 2010.

[14] Z. Suo. "Models for breakdown-resistant dielectric and ferroelectric ceramics" Journal of Mechanics and Physics Solids, vol. 41, pp. 1155-1176, 1993.